

## Controlling crystal orientation in microporous titanosilicate ETS-4 films by secondary growth method

B. YILMAZ, K. G. SHATTUCK, J. WARZYWODA, A. SACCO JR.\*

Center for Advanced Microgravity Materials Processing, Department of Chemical Engineering, Northeastern University, Boston, MA 02115, USA  
E-mail: [asacco@coe.neu.edu](mailto:asacco@coe.neu.edu)

Published online: 10 March 2006

During the last decade, there has been an increasing interest in the preparation of microporous and mesoporous films due to their potential use in a variety of applications. These include the conventional applications such as selective membranes, membrane reactors, chemical sensors, and fuel cells; as well as the novel applications in thermoelectric, optoelectronic and photovoltaic devices [1, 2]. ETS-4 is a crystalline microporous material with a tunable pore size between 3–4 Å, which is suitable for the separation of industrially important molecules [3]. Therefore, ETS-4 is a remarkable candidate for a diverse range of film applications. ETS-4 is a titanosilicate molecular sieve with a framework that contains [TiO<sub>6</sub>], octahedra forming linear monatomic ...Ti–O–Ti–O–Ti... chains, which are isolated from one another by a siliceous matrix made of [SiO<sub>4</sub>] tetrahedra [3, 4]. It has been hypothesized that these chains can behave as quantum wires [5–7]. The ...Ti–O–Ti–O–Ti... chains (“natural” quantum wires) in ETS-4 crystals run in the *b*-direction [8]. Hence, aligned ETS-4 crystals can function as oriented quantum wire arrays. ETS-4 has a unique one-dimensional pore channel system that is oriented in the *b*-direction [9, 10]. Thus, there is an interest in growing *b*-out-of-plane oriented ETS-4 films (crystal *b*-direction preferentially oriented normal to the substrate plane) for both conventional and novel applications.

Method of secondary (seeded) growth [11, 12], has been applied to fabricate ETS-4 films [10, 13, 14]. However, the effective conditions for direct hydrothermal synthesis of ETS-4 seed layers as well as controlling crystal orientation in ETS-4 films have not been identified to date. Control of the nucleation and crystal growth rates in secondary growth of seed layers is the key to achieve preferred orientation of the resulting films [11]. In this paper we have investigated the secondary growth mechanism of *b*-out-of-plane oriented ETS-4 films and established conditions to effectively decouple nucleation from crystal growth. The relatively low alkalinity of the synthesis mixtures allowed the first successful direct hydrothermal synthesis of ETS-4 seed layers on  $\alpha$ -alumina substrates.

Supported ETS-4 films were prepared utilizing a two-step hydrothermal synthesis procedure, which included direct crystallization of seed layers on supports followed by secondary growth of seed layers. Porous  $\alpha$ -alumina ( $\alpha$ -Al<sub>2</sub>O<sub>3</sub>, 30% void, ~0.7 mm thickness, CoorsTek) and titania (TiO<sub>2</sub>/TiO, 35–40% void, ~1 mm thickness, Atraverda) substrates were employed as supports. Previously, developed and investigated [5], synthesis mixtures with molar composition 3.6SiO<sub>2</sub>:1TiO<sub>2</sub>:5.5Na<sub>2</sub>O:4.4H<sub>2</sub>SO<sub>4</sub>:230.2H<sub>2</sub>O were used. Experimental details for preparation of a typical synthesis mixture and post-synthesis product recovery can be found elsewhere [5]. Rectangular substrates (~25 × ~5 mm) were diagonally placed in 10 ml Teflon-lined stainless steel autoclaves. Both faces of these rectangular substrates had identical surface characteristics, hence the diagonal placement of the substrates was random. Syntheses were carried out at 448 K for 72 hr. Seed layer syntheses were performed under autoclave rotation (72 rpm), whereas static hydrothermal conditions were used for secondary growth of these seed layers. Field emission scanning electron microscopy (FE-SEM, S-4700, Hitachi), X-ray powder diffraction (XRD, D5005, Bruker), and energy dispersive X-ray spectroscopy (EDX, Phoenix X-ray analyzer, EDAX) were used for characterization.

Seed layers were obtained on both substrate types (i.e.,  $\alpha$ -alumina and titania). XRD analysis confirmed that the seed layers consisted of ETS-4 crystals (Fig. 1b, d). This is the first successful direct hydrothermal synthesis of ETS-4 seed layers on  $\alpha$ -alumina substrates. This is likely due to the relatively low alkalinity (initial pH = 11.50 [5]) of the synthesis mixtures utilized. FE-SEM and EDX analyses demonstrated that the seed layers fully covered both sides of the substrates (Figs 2 and 3). There were intercrystalline gaps on the surfaces of these seed layers (Figs 2a and 3a). FE-SEM analysis showed that the seed layer thickness did not exceed 4  $\mu$ m (Figs 2b and 3b). XRD patterns of ETS-4 seed layers (Fig. 1b, d) were compared to the XRD pattern of ground, bulk ETS-4 particles (Fig. 1a).

\* Author to whom all correspondence should be addressed.

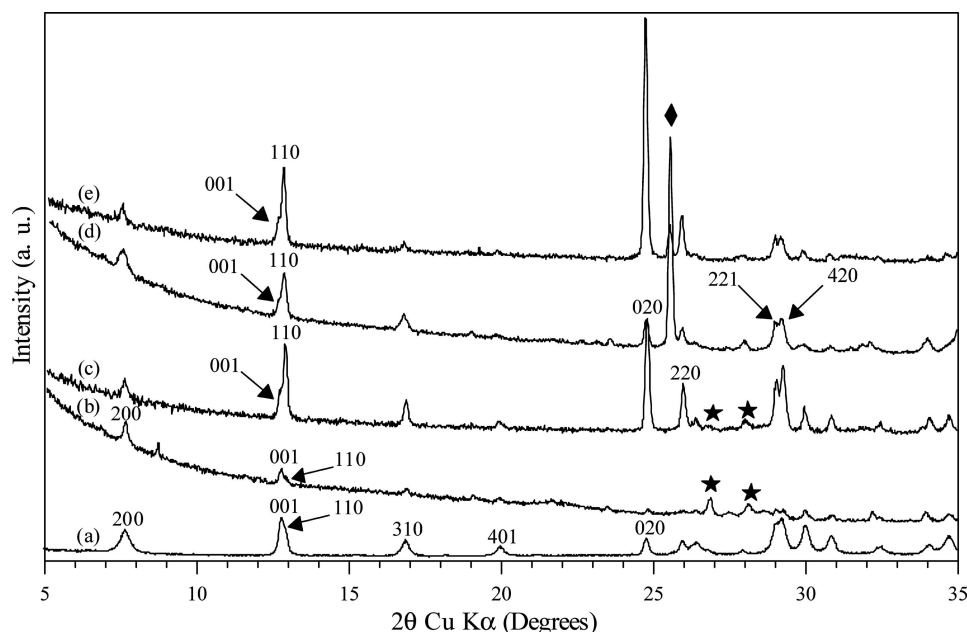


Figure 1 XRD patterns of (a) ground bulk ETS-4; (b) ETS-4 seed layer on titania substrate; (c) ETS-4 film on titania substrate; (d) ETS-4 seed layer on  $\alpha$ -alumina substrate; (e) ETS-4 film on  $\alpha$ -alumina substrate. Star and diamond symbols mark reflections due to titania and  $\alpha$ -alumina substrates, respectively.

For  $\alpha$ -alumina substrates, this comparison demonstrated that the (110)/(001) peak intensity ratio of ETS-4 in the seed layers increased (Table I), and the (110), (020), (220), (221), and (420) reflections dominated the XRD pattern (Fig. 1d). This indicates that the ETS-4 seed layers on  $\alpha$ -alumina substrates were partially *b*-out-of-plane oriented. To our knowledge, this represents the first preferentially oriented ETS-4 seed layer reported to date.

In contrast, the (200) and (001) reflections of ETS-4 dominated the XRD patterns of seed layers synthesized on titania substrates (Fig. 1b). Moreover, as illustrated in Table I, the (110)/(001) peak intensity ratio of ETS-4 in seed layers formed on titania substrates was much lower compared to the ground bulk sample. Thus, a large number of ETS-4 crystals on titania substrates appeared to be oriented with their *a*- or *c*-directions perpendicular to the substrate plane. Consistent with this was the substantial decrease of the intensities of the (020) reflection and other reflections corresponding to crystallographic planes, whose directions are nearly parallel to the crystal *b*-direction (Fig. 1b). Hence, the seed layers on titania substrates can be described as partially (*a*, *c*)-out-of-plane oriented.

TABLE I The (110)/(001) peak intensity ratios of ETS-4 crystals in samples synthesized in this study

Sample type	(110)/(001) peak intensity ratio*
Ground bulk ETS-4	$1.2 \pm 0.2$
ETS-4 seed layers on titania substrate	$\ll 1$
ETS-4 film on titania substrate	$3.2 \pm 0.2$
ETS-4 seed layers on $\alpha$ -alumina substrate	$2.8 \pm 0.3$
ETS-4 film on $\alpha$ -alumina substrate	$3.8 \pm 0.3$

\*Obtained by deconvolution of the peaks.

In the secondary growth step, ETS-4 films with thicknesses up to  $11 \mu\text{m}$  were obtained on both substrate types (i.e.,  $\alpha$ -alumina and titania) (Figs 4 and 5). Complete coverage on both sides of the substrates (i.e., top and bottom) was achieved. XRD patterns of final ETS-4 films (Fig. 1c, e) were compared to the XRD patterns of ground, bulk ETS-4 particles (Fig. 1a) and ETS-4 seed layers (Fig. 1b, d). For both substrate types, relative intensities of the (110), (020), and (220) reflections in the XRD patterns of ETS-4 films increased compared to those characterizing ground bulk crystals as well as seed layers. Furthermore, the (110)/(001) peak intensity ratios of ETS-4 films increased compared to those of seed layers (Table I). These findings indicated that highly *b*-out-of-plane oriented films were obtained on both  $\alpha$ -alumina and titania substrates. This is the first successful hydrothermal synthesis of preferentially oriented ETS-4 films on  $\alpha$ -alumina substrates. Previously, ETS-4 films could not be obtained on porous  $\alpha$ -alumina supports without incorporation of an impurity phase (i.e., Analcime) due to the dissolution of the support in the highly alkaline mixtures employed [10, 13, 14]. Utilization of a synthesis mixture with a relatively lower alkalinity (initial pH = 11.50) explored here allowed the growth of ETS-4 layers without the formation of an aluminosilicate material. Although the seed layers on each substrate type differed in orientation (partially *b*-out-of-plane oriented on  $\alpha$ -alumina versus partially (*a*, *c*)-out-of-plane oriented on titania), the final film orientation on both substrate types was the same (preferential *b*-out-of-plane orientation). This indicates that final orientation of the films studied is primarily related to the secondary growth conditions and is less dependent on the seed layer orientation.

Top view FE-SEM images (Figs 4a and 5a) revealed the increased dimensions of crystals on the film surface

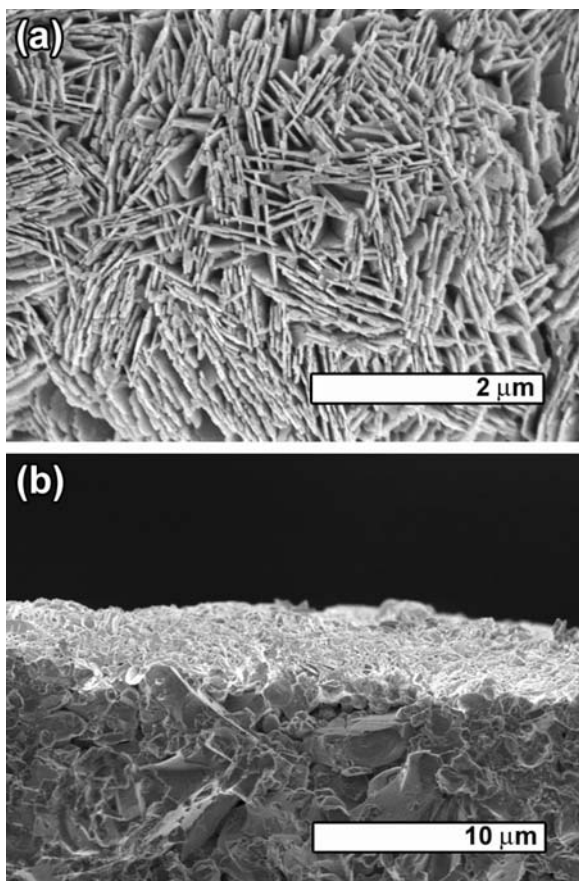


Figure 2 FE-SEM images of ETS-4 seed layer on  $\alpha$ -alumina substrate (a) top view; (b) cross-sectional view.

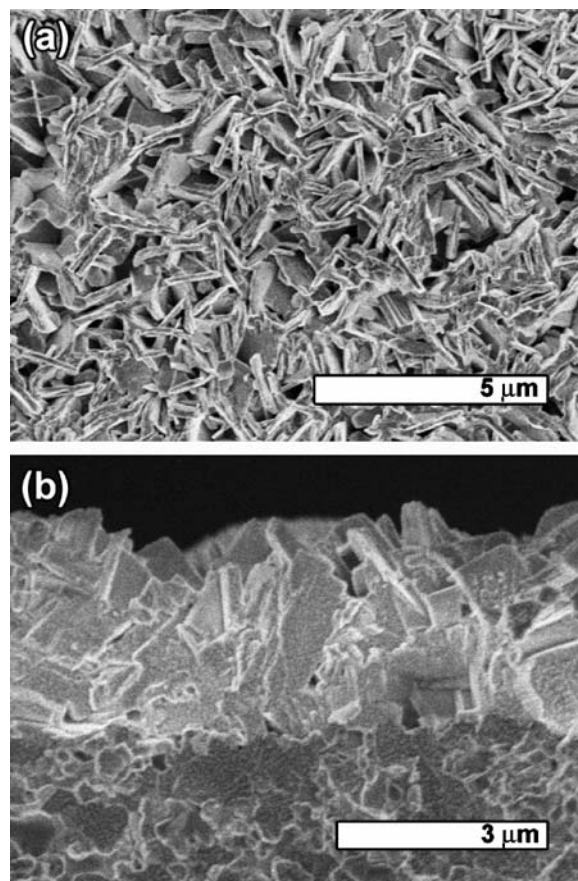


Figure 3 FE-SEM images of ETS-4 seed layer on titania substrate (a) top view; (b) cross-sectional view.

compared to the dimensions of seed crystals (Figs 2a and 3a). Cross-sectional FE-SEM analysis of the ETS-4 films on both substrate types showed columnar microstructures (Figs 4b and 5b). Columnar microstructures suggest that the seed crystals grew directly by epitaxy without incorporation of crystals nucleated in the solution phase of synthesis mixtures used in the secondary growth step [11]. Columnar microstructure and the increased degree of out-of-plane orientation in final films, together with the increased in-plane crystal dimensions indicate that the evolutionary selection mechanism of the van der Drift growth model [12, 15, 16] must have played a central role in the ETS-4 film development investigated here.

Theoretically, for preparation of oriented zeolite/zeotype films by secondary growth of seed layers, secondary growth conditions must lead to lower nucleation rate compared to crystal growth rate, and to highly anisotropic growth rates with the fastest growth along the direction of desired out-of-plane film orientation [11]. Traditionally, clear/dilute solutions characterized by low supersaturation levels have been used to decouple nucleation from crystal growth [10]. However, due to dilution, these solutions decrease the rates of both processes. This results in poorly developed films where intercrystalline gaps in seed layers still exist after the secondary growth step [10]. In order to improve the film continuity and/or

orientation, multiple secondary growth steps or longer processing times are necessary [10, 11]. Our results show that the synthesis mixtures utilized in this study effectively decoupled nucleation from crystal growth in the secondary growth step, and thus exclusively allowed growth of seed crystals that resulted in highly oriented ETS-4 films. These findings demonstrate that, contrary to the conventional low supersaturation approach to conducting secondary growth of seed layers, a synthesis mixture with very high supersaturation levels [5] can provide exceptional secondary growth conditions. The advantage of this synthesis mixture likely stems from the kinetics of ETS-4 crystallization. Crystallization curve of ETS-4 synthesized from this synthesis mixture [5] exhibits a long induction period, i.e., time prior to the start of nucleation. The high crystallization rate of ETS-4 from this composition [5], indicates a high driving force for crystal growth. In the secondary growth step, during the long induction period nutrients are solely consumed for the growth of crystals in seed layers. The highly anisotropic growth rates of ETS-4 crystals [8, 17], that provide the fastest growth along the *b*-direction are also critical in the synthesis of *b*-out-of-plane oriented ETS-4 films. This anisotropy gives ETS-4 a “self-orienting” characteristic during film development that results in preferential *b*-out-of-plane crystal orientation.

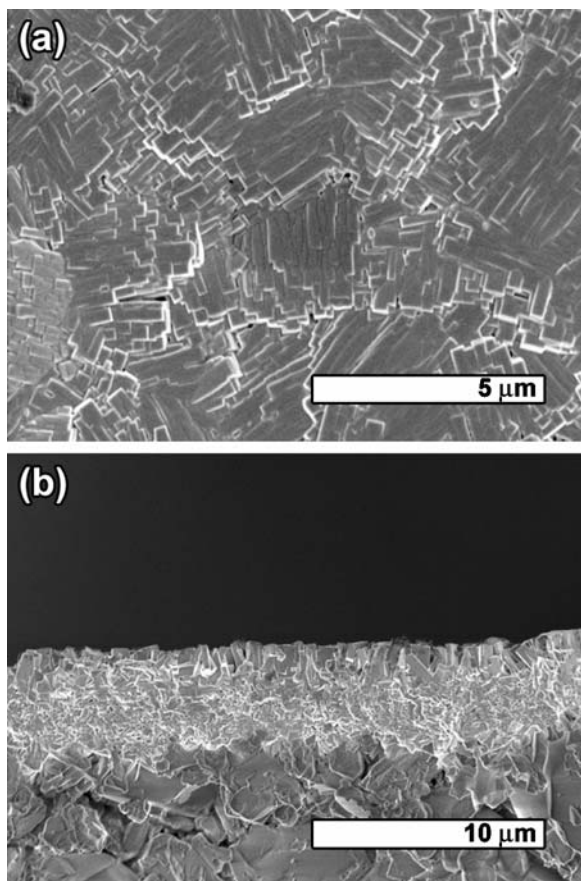


Figure 4 FE-SEM images of ETS-4 film on  $\alpha$ -alumina substrate (a) top view; (b) cross-sectional view.

In conclusion, the secondary growth conditions identified here, which effectively decouple nucleation from crystal growth, and at the same time provide the fastest growth along the *b*-direction, offer a promising approach for fabrication of *b*-out-of-plane oriented ETS-4 films. This method can be used for oriented ETS-4 film growth on a variety of substrates desirable for advanced applications. In addition, the low alkalinity of the synthesis mixture investigated is beneficial for seed layer/film fabrication on pH sensitive supports.

### Acknowledgments

The authors acknowledge NASA for financial support.

### References

1. H.-K. JEONG, J. KROHN, K. SUJAOTI and M. TSAPATSIS, *J. Amer. Chem. Soc.* **124** (2002) 12966.
2. H. W. HILLHOUSE and M. T. TUOMINEN, *Micropor. Mesopor. Mater.* **47** (2001) 39.
3. S. M. KUZNICKI, V. A. BELL, S. NAIR, H. W. HILLHOUSE, R. M. JACUBINAS, C. M. BRAUNBARTH, B. H. TOBY and M. TSAPATSIS, *Nature* **412** (2001) 720.
4. S. NAIR, H.-K. JEONG, A. CHANDRASEKARAN, C. M. BRAUNBARTH, M. TSAPATSIS and S. M. KUZNICKI, *Chem. Mater.* **13** (2001) 4247.

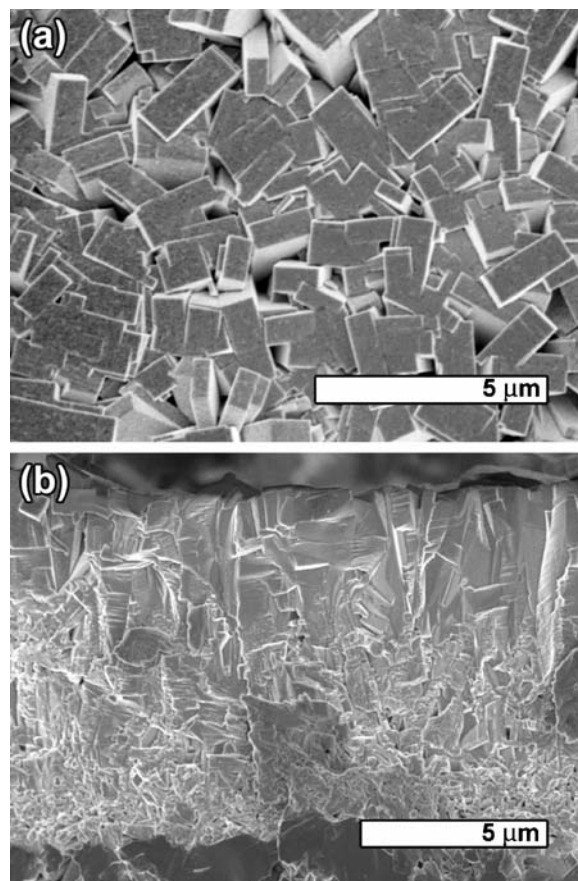


Figure 5 FE-SEM images of ETS-4 film on titania substrate (a) top view; (b) cross-sectional view.

5. B. YILMAZ, P. Q. MIRAGLIA, J. WARZYWODA and A. SACCO JR., *Micropor. Mesopor. Mater.* **71** (2004) 167.
6. J. WARZYWODA, B. YILMAZ, P. Q. MIRAGLIA and A. SACCO JR., *ibid.* **71** (2004) 177.
7. B. YILMAZ, J. WARZYWODA and A. SACCO JR., *J. Crystal Growth* **271** (2004) 325.
8. P. Q. MIRAGLIA, B. YILMAZ, J. WARZYWODA and A. SACCO JR., *ibid.* **270** (2004) 674.
9. C. BRAUNBARTH, H. W. HILLHOUSE, S. NAIR, M. TSAPATSIS, A. BURTON, R. F. LOBO, R. M. JACUBINAS and S. M. KUZNICKI, *Chem. Mater.* **12** (2000) 1857.
10. C. M. BRAUNBARTH, L. C. BOUDREAU and M. TSAPATSIS, *J. Membr. Sci.* **174** (2000) 31.
11. A. GOUZINIS and M. TSAPATSIS, *Chem. Mater.* **10** (1998) 2497.
12. G. XOMERITAKIS, S. NAIR and M. TSAPATSIS, *Micropor. Mesopor. Mater.* **38** (2000) 61.
13. G. GUAN, K. KUSAKABE and S. MOROOKA, *ibid.* **50** (2001) 109.
14. Idem., *Sep. Sci. Technol.* **37** (2002) 1031.
15. P. SMEREKA, X. LI, G. RUSSO and D. J. SROLOVITZ, *Acta. Mater.* **53** (2005) 1191.
16. C. V. THOMPSON, *Annu. Rev. Mater. Sci.* **30** (2000) 159.
17. P. Q. MIRAGLIA, B. YILMAZ, J. WARZYWODA and A. SACCO JR., *Micropor. Mesopor. Mater.* **69** (2004) 71.

Received 15 August  
and accepted 14 September 2005